Development of an automatic procedure for the characterization of silicon photomultipliers

Claudio Piemonte, *Member, IEEE*, Alessandro Ferri, Alberto Gola, Antonino Picciotto, Tiziana Pro, Nicola Serra, Alessandro Tarolli and Nicola Zorzi

***Abstract*– In this paper, we show the analysis software we created for a fast and reliable automatic characterization of a silicon photomultiplier. The program can be used both in dark and under continuous low-level light illumination. It grabs 1ms-long waveforms, each containing many single cell pulses, from an oscilloscope connected to the PC via Ethernet. On-line data analysis is done both on the raw waveform as well as on a filtered (with DLED technique) version in order to facilitate the pulse identification and the extraction of some parameters also in cases of high count rates or cross-talk. The main outcomes of the program are: single-cell signal shape, gain, primary dark count rate, after-pulse probability, direct and delayed cross-talk probability and excess charge factor. It can be used also to determine the actual photo-detection efficiency with the proper hardware set-up.**

I. Introduction

FBK has been developing silicon photomultipliers (SiPM) since 2006 [1]. Different technologies and designs have been implemented since that time with the aim of improving the device performance. The optimization process is quite time consuming since it involves many phases: process/device simulation, design, fabrication technology definition, production in the silicon micro-fabrication facility and characterization.

The latter phase, in turn, develops in different stages. For each fabricated lot, the first step is the measurement of the forward and reverse current which is done at the wafer level on automatic probe-stations. This is done to identify SiPMs with anomalous behavior. Then, after dicing, a number of samples are packaged and tested, first, in dark and, then, under illumination. In particular, the dark characterization can be quite time consuming in case of newly developed technologies since it has to be carried out at different bias and environmental (mainly temperature) conditions. In addition, the set of parameters to be measured in each situation is large. It includes: primary dark rate, after-pulse and optical cross-talk probabilities, gain and single-cell signal shape. A reliable hardware set-up and an automated acquisition procedure is mandatory to reduce testing time and produce meaningful data for the comparison of different technologies.

In this paper we focus on the acquisition software describing, in detail, the techniques we developed during the years for the extraction of the main parameters mentioned above. The tool is very effective since it allows a fully automated testing at different over-voltages and temperatures in a matter of few hours. It is interesting to note that the same acquisition set-up can be used also for the evaluation of the photo-detection efficiency under continuous light illumination.

Manuscript received November 16, 2012. This work has been partially supported by the EU FP7 project SUBLIMA, Grant agreement no. 241711.

C. Piemonte, A. Ferri, A. Gola, A. Picciotto, T. Pro, N. Serra, A. Tarolli and N. Zorzi are with Fondazione Bruno Kessler, Trento, Italy (telephone: +39 0461314428, e-mail: piemonte@fbk.eu).

II. Experimental Setup

The hardware set-up we use for signal acquisition and dark characterization is shown in Fig. 1. It consists of a light-tight thermostatic chamber containing the silicon photo-multiplier and the amplification stage. The temperature can be adjusted between -50 °C and 80 °C. It is controlled by the acquisition PC via a RS232 connection.

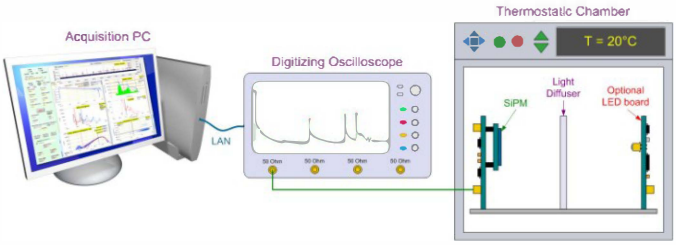

Fig.1. Sketch of the hardware set-up. It is composed by a climatic chamber housing the SiPM with its amplifier, a digital oscilloscope and a PC acquiring the data via Ethernet connection.

The amplifier output signal is acquired by a digital oscilloscope. The scope (Agilent DSO9104A) is set to acquire 1ms-long waveforms with a sampling rate of 10 GS/s. The bandwidth is set to 500 MHz. The digitized data is sent via Ethernet connection to the acquisition PC for the on-line analysis. The waveform acquisition and analysis is repeated iteratively to accumulate the desired statistics for the different parameters at a given bias and temperature condition. A LabView program takes care of all the setting conditions as well as data acquisition/analysis.

The schematic of the amplifier board is shown in Fig. 2. It has been designed by FBK and consists of a low-noise, high-bandwidth voltage-feedback operational amplifier with JFET input, connected in a trans-impedance configuration. The low bias-current input stage and the use of an inverting configuration preserve the total signal charge of the SiPM pulses, despite the possible OPA non-idealities like, e.g., its slew rate. The feedback resistor has a value of 2 kΩ, providing a sufficient gain for the analysis of the single cell pulses.

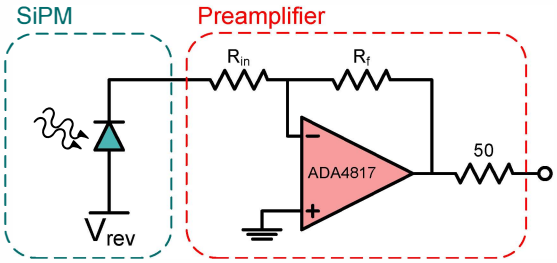

Fig.2. Discrete analog amplifier used to couple the SiPM to the oscilloscope.

In the following, the automatic characterization procedure is fully described with the aid of measurements. In particular, we show results from an FBK SiPM featuring a technology developed in 2006. The device is 1x1 mm^2 with a cell size of 50x50 μm^2. In order to better describe the features of the program the measurement temperature is set at -20 °C while the over-voltage spans in a very wide range (about 10 V).

III. On-line Software Algorithm

Once the temperature and bias conditions are set by the program, the waveform acquisition gets started. As already mentioned, 1 ms-long data sets are acquired. Several dark pulses are expected to fall into this timeframe: in the order of 1000 for a dark rate of 1 MHz.

The first step consists of a signal manipulation in order to reduce the single cell pulse width. This is important to minimize the pile-up probability which can make the pulse identification difficult. Furthermore, on piled-up signals, the amplitude of each pulse is not assigned correctly. The filtering technique used in this implementation is called DLED [2] and was developed to optimize the timing resolution capability of SiPMs coupled to scintillators. The DLED waveform is obtained subtracting to the original waveform a delayed (500 ps) replica. In this way, only the fast rising edge of each signal is preserved while the long tail is strongly suppressed. The DLED signal can have a pronounced undershoot if the SiPM signal has a fast decay component [1]. A further step, explained hereafter, is performed to get rid of it. A pulse identification procedure is launched: an array containing the time stamps of the events having a peak above a threshold (set at half the amplitude of the single cell response) is created. An average DLED pulse (about 500ns long) is determined considering only independent events well separated in time, i.e. with a time stamp far enough (>1 μs) from previous and subsequent ones. This average pulse is used to subtract the undershoot in the DLED waveform at each time stamp. The pulse identification procedure is then repeated on the new waveform to check whether there were missing time stamps because of events falling in the undershoot. If this is the case, the undershoot correction is repeated on the new events discovered. This relatively complicated procedure is very effective and allows a correct waveform analysis also in cases of high dark count and/or correlated noise.

An example of a difficult case is given in Fig. 3, showing a fraction of a waveform. The red line is the original signal. There is a first single cell pulse followed by other piled-up events some of them probably due to cross-talk. It is clearly difficult to identify the pulses and assign them the correct height. The blue line is the waveform resulting from the DLED filtering + undershoot compensation. Each pulse has now a duration of few ns so the complicated situation is easily resolved: three singles and one double signal are visible.

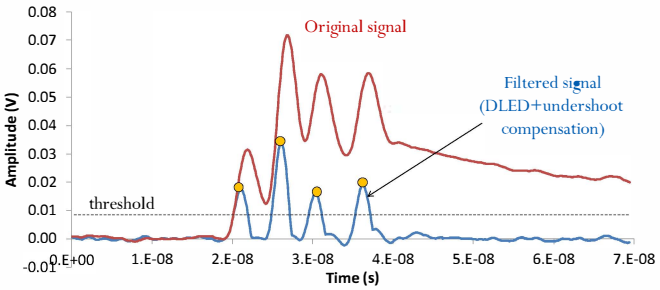

Fig.3. Example of a critical situation (red line) extracted from an acquired waveform and its filtered version (blue line) showing the single components of the original complicated structure.

After this initial phase, a number of waveforms are acquired and processed. The DLED signal is used to characterize the noise whereas the original signal is used to determine the gain and signal shape. At each acquisition the waveforms are analyzed and relevant data accumulated in arrays.

A. Analysis of DLED signal

When all the events in a waveform are identified with a time stamp, two arrays are created: one containing the time distance between consecutive events and a second containing the pulse amplitudes corresponding to the time stamps. The combination of the two arrays includes all the relevant information regarding the noise of the device and it is represented in the scatter plot of Fig. 4.

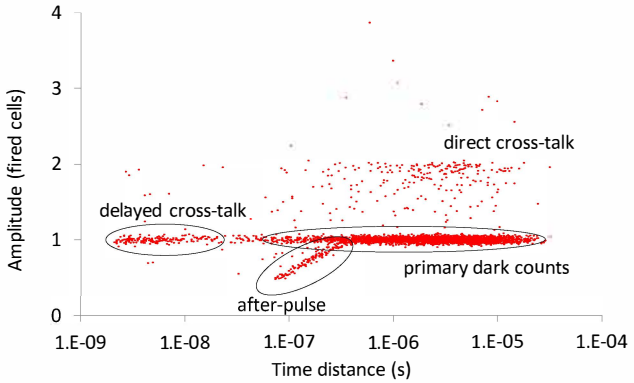

Fig.4. Scatter plot of the pulse amplitude as a function its distance from the preceding event at 7.2V over-voltage.

Each point in the plot is the amplitude of an event as a function of its distance from the preceding one. The pulse amplitude is normalized to the height of the single-cell signal. All the different noise components are visible:

- cloud of dots with amplitude around 1 and located between 30 ns and 50 µs are primary dark events. The density of this cloud follows a Poisson distribution as will be shown later on;
- dots with amplitude between 0.5 and 1 and located between 50 and 200 ns are after-pulses. After-pulses with amplitude less than 0.5 are not found because the threshold for the pulse identification is set at that value. After-pulses can have amplitude equal to 1 when the distance from previous pulse is longer than 200 ns. These cases can be identified as shown later.
- dots with amplitude 2 or 3 correspond to "direct" optical cross-talk events. In these cases, during a primary cell discharge, a photon is emitted and absorbed in the depletion region of a neighboring cell triggering a second discharge in coincidence with the first one. The density of dots above the primary DCR cloud also follows the Poisson distribution.
- Cloud of dots with amplitude 1 located at very short time distances (between 5 and 20ns) are related to "delayed" cross-talk. In these cases, during a primary cell discharge, a photon is emitted and absorbed in the non-depleted region beneath a neighboring cell triggering a second discharge with a certain delay from the first due to the diffusion time of the photo-generated carrier.

Quantitative information about the noise components can be extracted from the histograms of the two arrays, i.e. the projections of the scatter plot on the two axis.

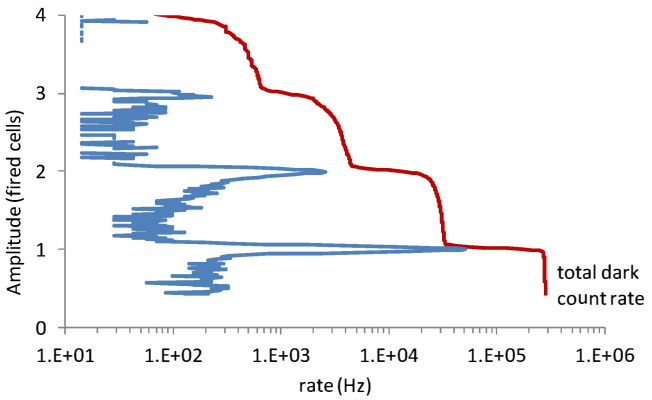

Fig.5. Histogram of the amplitude array, i.e. projection of the scatter plot on the y axis at 7.2V over-voltage.

Fig.5 shows the histogram of the amplitude array (blue line). To be consistent with the representation of Fig. 4, the amplitude is on the y scale whereas frequency is on the x scale. The latter is expressed in Hz and calculated as the average number of events found in each of the waveforms analyzed divided by the waveform duration (1ms). In red, the cumulative histogram is shown. From this plot we extract the Total Dark Count Rate (DCR_{tot}) as the highest cumulative rate. It includes primary dark noise, after-pulses with height higher than 0.5 and delayed cross-talk. From the plot, it is possible to measure the amount of optical cross-talk in the device. We can assume that every event has a probability p of generating a single secondary cross-talk event. Therefore, p can be obtained from the ratio between the areas of the peaks corresponding to the double and single events. The same value can be obtained from the ratio between areas of the third and second peaks and so on.

In a more accurate model for the cross-talk [3], every event directly generates a Poisson distributed number of events, with mean value N_{ct}. Accordingly, the cross-talk is modeled as a branching Poisson process, and the total number of events, X, generated by a primary dark count, follows the Borel distribution. The expected value for X is $1/(1-N_{ct})$. From the plot in Fig.5 it is also possible to estimate the value of N_{ct}, even though for relatively low values of p and N_{ct}, the two methods are expected to be in good agreement.

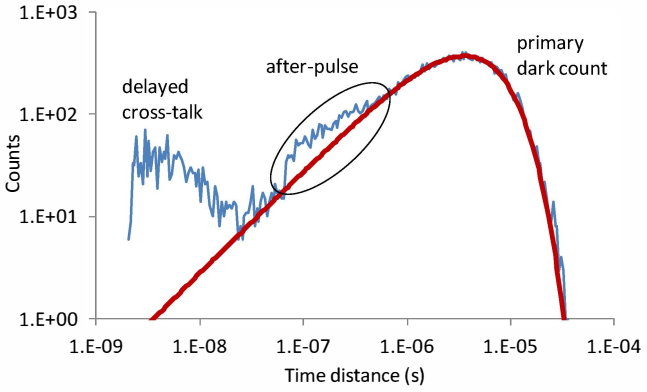

Fig.6. Histogram of the time delay array, i.e. projection of the scatter plot on the x axis at 7.2V over-voltage.

Fig. 6 shows the histogram of the time delay array (blue line). Both the x scale and the time binning are logarithmic. This representation is very convenient because in one plot we can see the different components in the whole time scale. The red line is the Poissonian fit of the primary dark events distribution. The position of the maximum is the inverse of the Poisson rate (DCR). At short time distances we see two distinct bumps deviating from the Poisson fit. Around 100ns we have the after-pulse (AP) bump, which, from the scatter plot on Fig. 4, are events with amplitude from 0.5 to 1. The AP probability is calculated as the ratio between the counts in excess of Poissonian fit, above 50 ns, and the total rate. The bump around 10 ns is related to delayed cross-talk (DeCT). DeCT events are confined in the first 20 ns, meaning that above this time the photo-generated carrier recombines before reaching the depletion region. As for AP, its probability can be calculated as the ratio between the counts in excess of Poisson fit, from 5 ns to 30 ns, and the total rate. The two phenomena can be clearly separated because, being the threshold set at 0.5 amplitude, after-pulses cannot occur at time distance below 50ns.

It is interesting to note that the same method, and thus acquisition program, can be used to count photons in a situation of constant light illumination. Indeed, the Poisson fit allows to have a counting free from correlated noise. It can be used therefore to measure the photo-detection efficiency of the SiPM.

B. *Analysis of original signal*

After the completion of the DLED waveform analysis, the program switches to the original data. The information extracted in this phase are the cell gain and signal shape.

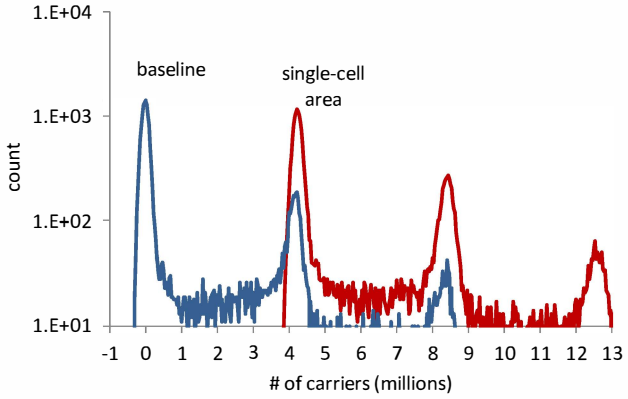

Fig.7. Area of the waveform (1 μs integration time) after the time stamp (red line) and before (blue line) at 7.2 V over-voltage.

For the first parameter, the procedure is the following. The array containing the time stamps is used to identify the pulses in the original waveform. Two sets of arrays are created containing the area of a portion of the waveform after and before each timestamp, respectively. The integration time can be varied according to the duration of the pulse. The first array contains the SiPM pulse areas whereas the second contains mainly information on the baseline. Fig. 7 shows the histograms of the two arrays. The x scale is expressed in number of carriers: it can be extracted from the area value (V·s) once the gain of the amplifier is known. The gain is the distance between the single-cell area and the baseline peak.

Once the signal histogram (red plot of Fig. 7) is well defined, it is possible to extract the shape of the single cell response with the following procedure. First, the timestamps corresponding to events having an area falling in the very proximity of the single-cell peak are selected. Then, 1 μs long portions of the waveform following those timestamps are averaged. The resulting signal shape is the red line in Fig. 8. It presents a fast component and a perfectly exponential recovery.

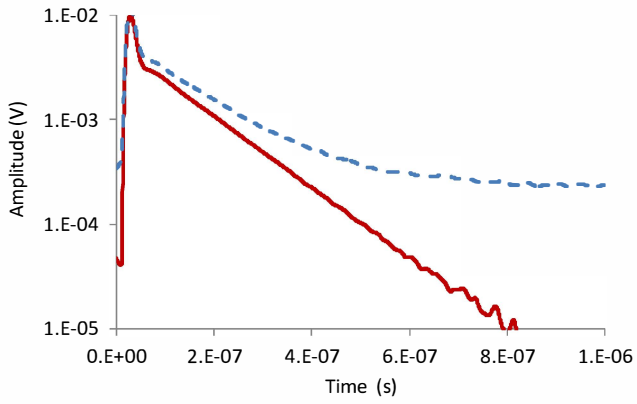

Fig.8. Average of the single cell signal response of events with area falling in the first peak of Fig. 7 (red line) and average of all events (blue line).

Fig. 8 shows also the signal obtained averaging the waveform portion following all the timestamps. This signal has a clearly longer tail due to the random presence of other pulses in the average window.

Finally, a last important parameter can be extracted combining the two analysis: the excess charge factor (ECF). The ECF gives information about the average excess charge associated to a primary event. It is manly related to correlated noise such as optical-cross talk and after-pulsing, but it can also be related to other sources of additional charge, such as a non-perfect quenching mechanism. In an ideal device, without correlated noise, it should be equal to one. The evaluation of this parameter is straightforward once the dark reverse current (I_{DC}), the primary dark count rate (DCR) and the single cell gain (G) at a given bias voltage are known. Indeed,

$$I_{DC}(V) = q \cdot G_{eq}(V) \cdot DCR(V) = q \cdot G(V) \cdot ECF(V) \cdot DCR(V) \quad (1)$$

where q is the electron charge, G_{eq} is an equivalent gain factor, and V is the bias voltage. This parameter is extremely important because it is linked to the multiplication noise factor which is the main cause of the SiPM resolution degradation even if the single photon spectrum is clearly visible in case of very few photons.

IV. Off-line Data Analysis

The procedure described in the previous paragraph is performed at different over-voltages and relevant data are saved. Another LabView program loads the files and creates a summary of the device behavior at a certain temperature. Below, some results on the 1x1 mm^2 SiPM at -20 °C are shown.

Fig. 9 shows the cumulative histogram of the amplitude array at three over-voltages: 3.2, 7.2 and 10.2 V. As expected, both the total dark rate and the direct cross-talk increase with the voltage.

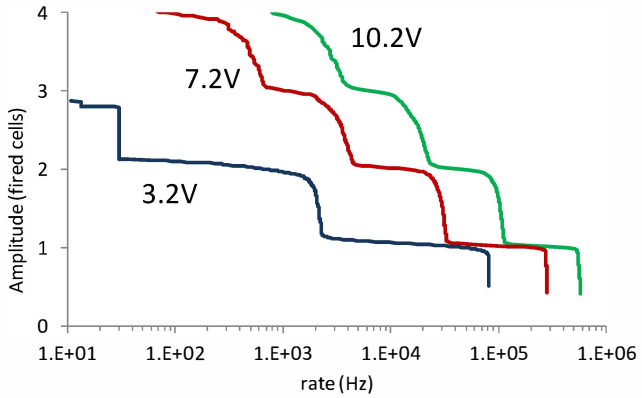

Fig.9. Histogram of the amplitude array at different over-voltages.

Fig. 10 shows the histogram of the time delay array at low and high over-voltages. The Poisson distribution clearly shifts towards shorter time distances with increasing voltage. On the other hand, the after-pulse and delayed optical cross-talk

bumps are always located at the same time position, but with reduced intensity at lower voltage.

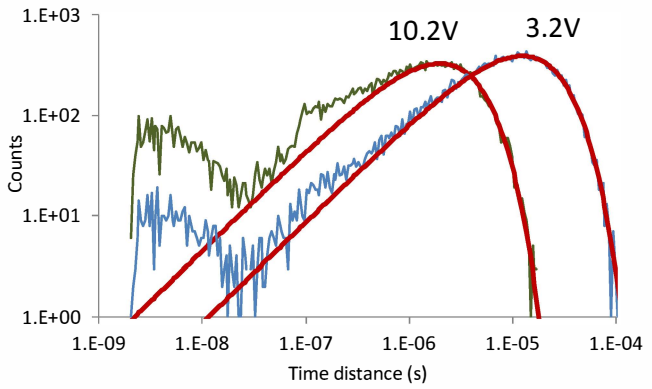

Fig.10. Histogram of the time delay array at low and high over-voltages.

The primary and total dark count rates are summarized in Fig. 11 for a set of bias voltages. Since the latter includes also after-pulses and delayed cross-talk events, it is increasingly higher with over-voltage than the first one.

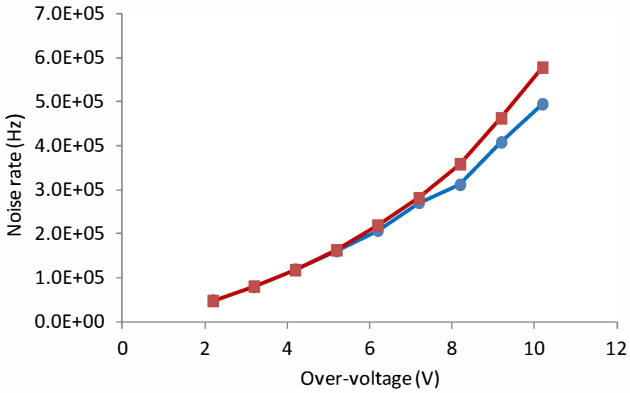

Fig.11. Total (red, squares) and primary (blue, circles) dark count rates as a function of over-voltage.

Fig. 12 shows the gain as a function of the over-voltage. The blue line (circles) is gain as calculated from the signal area whereas the red line (squares) is gain extracted from the current (G_{eq}). The latter is not linear and it is steadily increasing compared to the single cell gain. This means that the excess charge associated to a primary event increases because of a higher correlated noise. On the other hand, at low over-voltages they are well matching.

The excess charge factor, calculated as the ratio of the two lines in Fig. 12, is shown in Fig. 13. At 6V over-voltage the ECF is below 1.15.

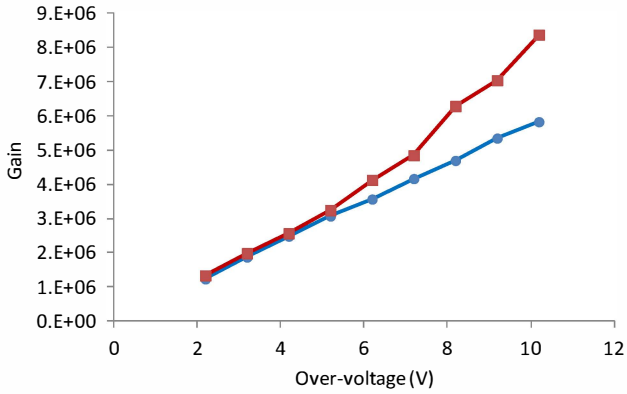

Fig.12. Gain vs. over-voltage calculated from the area of single pulses (blue, circles) and DC current (red, squares).

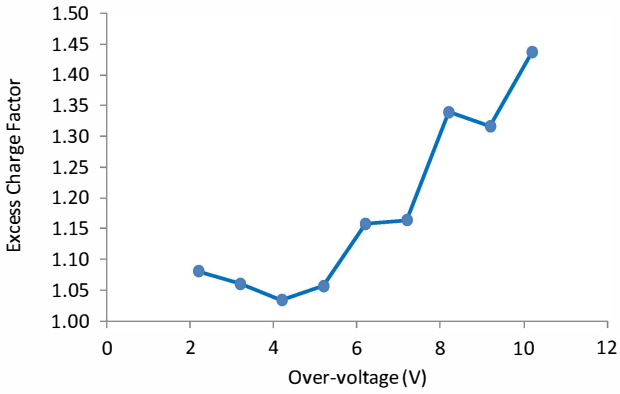

Fig.13. Excess charge factor as a function of the of the over-voltage.

V. Conclusions

In this paper we presented a fully automatic procedure for the characterization in dark of silicon photomultipliers. The program allows to get, in a very short time, a full picture of the device characteristics in terms of primary and correlated noise, gain, signal shape and excess charge factor. This application is extremely useful when a relatively high number of devices, also fabricated with different technologies, has to be measured and compared. The same program can be used to evaluate the photo-detection efficiency of the device.

VI. References

[1] C. Piemonte et al., "Characterization of the first silicon photomultipliers fabricated at ITC-irst ", *IEEE Transactions on Nuclear Science*, vol. 54, N. 1 pp. 236-244, February 2007.

[2] Gola, A.; Piemonte, C.; Tarolli, A.; , "The DLED Algorithm for Timing Measurements on Large Area SiPMs Coupled to Scintillators," IEEE TNS, vol.59, no.2, pp.358-365, April 2012.

[3] S. Vinogradov, "Analytical models of probability distribution and excess noise factor of solid state photomultiplier signals with crosstalk", NIMPR A, Vol. 695, 2012, pp. 247-251.